THE CANADIAN MINERALOGIST

A RE-EXAMINATION OF THE ARSENOPYRITE GEOTHERMOMETER: PRESSURE CONSIDERATIONS AND APPLICATIONS TO NATURAL ASSEMBLAGES*

ZACHARY D. SHARP, ERIC J. ESSENE AND WILLIAM C. KELLY

Department of Geological Sciences, The University of Michigan, Ann Arbor, Michigan 48109, U.S.A.

ABSTRACT

Experiments on the stability of arsenopyrite in the system Fe–As–S have led to the use of arsenopyrite compositions as a geothermometer (Clark 1960a,b, Kretschmar & Scott 1976), but the effect of pressure has not been resolved. Volume calculations show that pressure will shift sulfidation buffer-curves in the system Fe–As–S to higher sulfur fugacity $f(S_2)$. Increasing pressure will decrease the arsenic content of arsenopyrite coexisting with loellingite, and will increase the upper stability of arsenopyrite coexisting with pyrite by approximately 14°C/kbar. Partial molar volumes for arsenopyrite solid-solutions indicate that pressure has a negligible effect on the composition of arsenopyrite coexisting with pyrite, but sulfidation buffer-curves will be shifted to higher $f(S_2)$ by up to one log unit. If arsenopyrite $FeAs_{1-x}S_{1+x}$ lies on the FeS_2–$FeAs_2$ binary join, its composition should be fixed when buffered by either pyrite or loellingite alone at fixed P and T. Experiments on the ternary system Fe–As–S have been interpreted to show that two phases are required to fix the composition of arsenopyrite at any P and T (Kretschmar & Scott 1976), suggesting major deviations from ideality for arsenopyrite or possible errors in the experimental data. Application of the arsenopyrite geothermometer appears valid for deposits metamorphosed to greenschist and lower amphibolite facies (Oriental, Homestake: ~500°C inferred and calculated), but yields low temperatures for deposits metamorphosed to upper amphibolite and granulite facies (Balmat, Geco: ~650°C inferred, 500°C calculated), and inconsistent temperatures for low-temperature hydrothermal deposits (Panasqueira: ~300°C inferred, 500°C calculated).

Keywords: arsenopyrite, geothermometry, geobarometry, sulfide stability, sulfur fugacity, sulfide thermodynamics.

SOMMAIRE

Les données disponibles sur la stabilité de l'arsenopyrite dans le système Fe–As–S ont permis l'utilisation des compositions de ce minéral comme géothermomètre (Clark 1960a, b, Kretschmar & Scott 1976), mais l'influence de la pression restait méconnue. Le calcul des volumes montre qu'une augmentation de la pression déplace les courbes des assemblages-tampon dans les réactions de sulfidation du système Fe–As–S vers les fugacités plus élevées du soufre. Aussi, cette augmentation diminue la proportion de l'arsenic dans l'arsenopyrite qui coexiste avec loellingite, et augmente le champs de stabilité de l'arsenopyrite qui coexiste avec la pyrite d'environ 14°C/kbar. Les volumes molaires partiels pour les solutions solides d'arsenopyrite indiquent que la pression exerce un effet négligeable sur la composition de cette phase en coexistence avec la pyrite, mais la courbe de la réaction-tampon est déplacée à $f(S_2)$ plus élevée par un ordre de grandeur. Si l'arsenopyrite $FeAs_{1-x}S_{1+x}$ fait partie du système binaire FeS_2–$FeAs_2$, sa composition serait fixée par la seule présence de pyrite ou loellingite à P et T fixes. On déduit, à partir des résultats d'expériences dans le système ternaire Fe–As–S, que deux phases sont nécessaires pour fixer la composition de l'arsenopyrite en termes de P et T (Kretschmar & Scott 1976), ce qui laisse prévoir des déviations importantes de l'idéalité de l'arsenopyrite et des erreurs possibles dans les données expérimentales. L'application du géothermomètre paraît valide pour les gîtes minéraux métamorphisés aux facies schistes verts et amphibolite inférieur (Oriental, Homestake: 500°C, température déduite et calculée). Le géothermomètre donne des températures trop basses pour les gîtes métamorphisés dans les facies amphibolite supérieur et granulite (Balmat, Geco: température déduite 650°C, calculée 500°C) et des résultats erratiques pour les gisements hydrothermaux de basse température (Panasqueira: température déduite 300°C, calculée 500°C).

(Traduit par la Rédaction)

Mots-clés: arsenopyrite, géothermométrie, géobarométrie,

stabilité des sulfures, fugacité du soufre, analyse thermodynamique des sulfures.

INTRODUCTION

Many metamorphosed ore-deposits have significant economic importance (*e.g.,* Broken Hill, New South Wales; Homestake, South Dakota; Balmat, New York), and an understanding of their metamorphic history is warranted. Efforts to find sulfides suitable for geothermometry and geobarometry have been limited by the generally nonrefractory nature of this group of minerals. Arsenopyrite is one of the few sulfides, besides sphalerite, that is relatively refractory and exhibits appreciable solid-solution sensitive to pressure or temperature (Clark 1960a,b, Barton 1970, Scott 1974, 1976). Experiments on the stability of arsenopyrite in the system Fe–As–S (Clark 1960a,b, Barton 1969, Kretschmar & Scott 1976) were limited by extremely slow rates of reaction, precisely because of the refractory nature of arsenopyrite. We have evaluated the arsenopyrite geothermometer by analyzing natural assemblages whose P–T histories have previously been independently established. These include fluid-inclusion filling temperatures corrected for pressure, isotope fractionation and silicate phase-equilibria.

Ideal arsenopyrite ($FeAs_{1-x}S_{1+x}$, $x \leq |0.13|$) lies on the binary join pyrite (FeS_2) – loellingite ($FeAs_2$), although minor deviations from the stoichiometric ratio $Fe/(As + S) = \frac{1}{2}$ have been reported (Klemm 1965, Kretschmar & Scott 1976). The composition of ideal arsenopyrite is fixed at a given pressure and temperature when equilibrated with either pyrite or loellingite. Experiments on the binary join were carried out by Clark (1960a,b), who found that buffered arsenopyrite is enriched in arsenic with increasing temperature and enriched in sulfur with increasing pressure (Fig. 1). He concluded that the maximum stability of coexisting arsenopyrite and pyrite is approximately 490°C at 1 bar, but is extended to 520°C at 2 kbar. Kretschmar & Scott (1976) concluded that two Fe–As–S phases are needed to buffer arsenopyrite composition at a given pressure and temperature, and inferred that slight deviations from the ideal cation/anion ratio cause arsenopyrite to plot off the simple FeS_2–$FeAs_2$ binary join. Their experimentally determined graph of temperature *versus* at.% As in arsenopyrite is shown in Figure 2. Kretschmar & Scott (1976) were unable to duplicate the pressure dependence observed by Clark and proposed that the pressure effect on composition is less than Clark had reported. They suggested that the gold in the capsules that Clark had used for his experiments may have diffused into the arsenopyrite charge, and circumvented the problem by using glass-walled capsules (see Kretschmar 1973 for details).

PROCEDURE

Arsenopyrite-bearing samples from localities with accurate pressure–temperature estimates were analyzed quantitatively for Fe, As, S, Ni, Bi, Sb and Co using an ARL–EMX electron microprobe at the University of Michigan. Operating conditions were as follows: accelerating voltage 15 kV; beam current 150 μA; sample current on arsenopyrite 0.015 μA. A grain of analyzed arsenopyrite (asp 200) from Dr. S.D. Scott was used as a standard for Fe, As and S. Synthetic NiS, Co_3S_4, Sb_2S_3 and Bi metal were used as standards for the other elements. Each analysis consisted of a minimum of ten point-counts per grain at 20 seconds per point. Up to ten grains were analyzed within a single sample. Samples reanalyzed using arsenic metal and pyrite as standards for Fe, As and S gave comparable results. Volatilization and migration of elements were evaluated by successive measurements at a single point.

Unit-cell refinements of several samples of arsenopyrite were obtained to confirm the volume-composition data of Morimoto & Clark (1961). X-ray measurements were made with a powder diffractometer using Cu$K\alpha$ radiation, a graphite monochrometer and reagent-grade CaF_2 checked against quartz as an internal standard. A least-squares-refinement program after Burnham (1961) was used to calculate cell parameters of arsenopyrite, assuming a monoclinic cell.

RESULTS

For each locality, pressure–temperature estimates, buffering assemblages, and microprobe data are
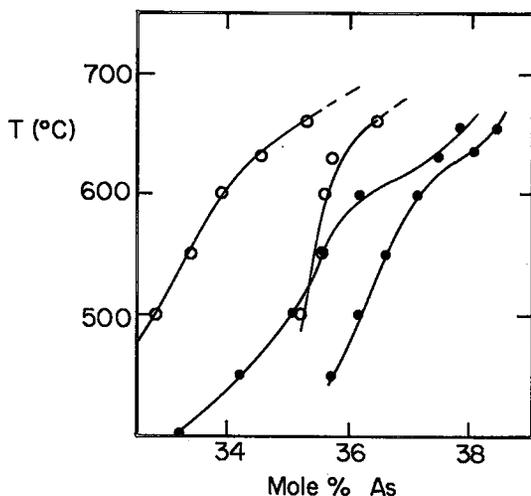
FIG. 1. Stability of arsenopyrite at 1 bar (open circles) and at 5 kbar (solid circles). Limbs of the stability field are for compositions stable with end-members pyrite (As-poor limb) and loellingite (As-rich limb). Compositions were determined from the d_{131} data of Clark (1960b) by using the composition equation from Kretschmar & Scott (1976).
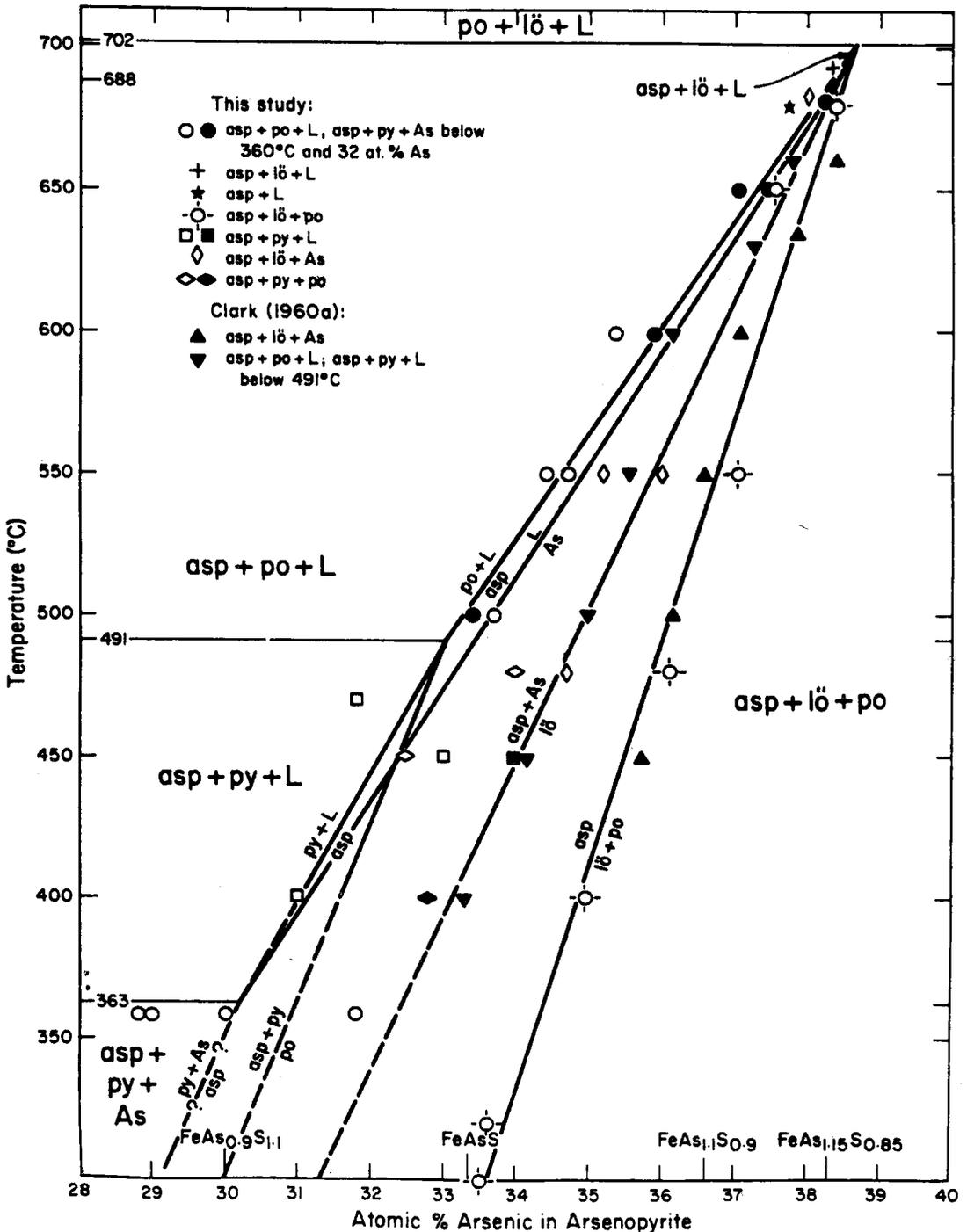
FIG. 2. T–X diagram with arsenopyrite-buffered curves (reprinted from Kretschmar & Scott 1976).

listed in Table 1. Microprobe data are reported to two significant figures to avoid rounding errors. A more complete description of each locality analyzed in this study is given in the section Analysis of Natural Assemblages. Compositions of arsenopyrite all lie close to the line representing the stoichiometric

TABLE 1. ARSENOPYRITE COMPOSITION, COEXISTING MINERALS IN THE Fe-As-S SYSTEM, AND P-T CONDITIONS OF FORMATION

Sample locality	comp. (wt.%)				comp. (at.%)			analyt. method	mineral assemb.	ref.	P (kbar)	T (°C)	ref.
	Fe	S	As	total	Fe	S	As						
Homestake, SD #6	35.18	20.63	45.42	101.23	33.51	34.23	32.25	EM	po-py(?)	(1)	2-3	500±50	(2,16)
" #7	34.11	19.73	46.60	100.44	33.30	33.65	33.30	EM	po	(1)	"	"	(2,16)
Oriental Mine, CA													
9-13-252	35.30	22.21	41.65	99.16	33.61	36.83	29.56	EM	po-py	(1)	0.2-1	490±40	(3)
9-15-112	35.76	22.20	42.91	100.87	33.60	36.34	30.06	EM	py	(1)	"	"	"
"	-	-	-	-	-	-	30.9	XR	"	(1)	"	"	"
Geco, Ontario	35.49	21.46	44.85	101.80	33.39	35.16	31.45	EM		(1)	6.0±0.1	650±30	(4)
Balmat, NY	33.52	21.10	45.58	100.20	32.15	35.26	32.59	EM	py	(1)	6.5±0.5	625±25	(5)
Araca, Bolivia[1]													
ARA-74[1]	34.79	20.45	46.16	101.40	33.19	33.98	32.83	EM	po	(1)	0.19-1.0	490±40	(6)
"	-	-	-	-	-	-	32.2	XR	"	(1)	"	"	"
"	-	-	-	-	-	-	32.8	XR	"	(6)	"	"	"
ARA-107[2]	31.80	18.17	48.56	100.93	31.31	31.20	35.63	EM	lo-po	(1)	"	"	"
ARA-58	33.4	17.1	48.5	99.0	33.6	33.0	36.4	EM	po	(7)	"	"	"
"	-	-	-	-	-	-	35.8	XR	"	(6)	"	"	"
Kalahuyo, Bolivia													
CHA-23	33.90	19.76	46.72	100.38	32.87	33.37	33.76	EM	po-py(?)	(1)	"	"	"
"	34.4	20.2	46.6	101.2	33.0	33.7	33.3	EM	"	(7)	"	"	"
"	-	-	-	-	-	-	33.5	XR	"	(1)	"	"	"
"	-	-	-	-	-	-	32.9	XR	"	(6)	"	"	"
Llallagua, Bolivia[3]	33.01	19.65	45.56	99.92	32.62	33.82	33.56	WC		(10)	"	"	"
Sayaquira, Bolivia													
SAY-14	34.5	20.0	46.4	100.9	33.2	33.5	33.3	EM	po	(7)	"	"	"
"	-	-	-	-	-	-	33.3	XR	"	(6)	"	"	"
SAY-27	34.2	19.7	46.7	100.6	33.1	33.2	33.7	EM	po-py	(7)	"	"	"
Tasna, Bolivia													
TSN-36	34.0	19.5	45.9	99.4	33.3	33.2	33.5	EM	po	(7)	"	"	"
"	-	-	-	-	-	-	33.8	XR	"	(6)	"	"	"
Panasqueira, Portugal													
PGL-5	34.26	18.44	48.99	101.69	33.29	31.22	35.49	EM	po-py(?)	(1)	<1.0	280±50	(8)
PGL-40	33.59	17.95	48.91	100.45	33.16	30.86	35.98	EM	"	(1)	"	"	"
PGL-217	34.04	18.10	48.95	101.09	33.36	30.89	35.75	EM	"	(1)	"	"	"
"	-	-	-	-	-	-	35.7	XR	"	(1)	"	"	"
PGL-244	33.71	17.58	49.43	100.72	33.32	30.26	36.42	EM	"	(1)	"	"	"
"	-	-	-	-	-	-	36.4	XR	"	(1)	"	"	"
PGL-303	34.16	18.16	48.30	100.62	33.56	31.07	35.37	EM	"	(1)	"	"	"
Timmins, Ont.													
P-23	35.02	22.74	41.75	99.51	33.11	37.46	29.43	EM	py	(1)	1.0-1.5	320±30	(15)
Cleveland Mine, Tasmania	-	-	-	-	-	-	33.6±1.0	XR	po	(9)	1.5±0.5	490±10	(9)
Moreton's Hrbr, Nfld.	34.1	19.9	45.3	99.3	33.3	33.8	32.9	EM	po-lo	(7)	1.2±0.3	350±50	(12)
"	-	-	-	-	-	-	32.5±2.5	EM	"	(12)	"	"	"
Broken Hill, NSW[4]	31.8	17.1	50.0	98.9	32.2	30.1	37.7	EM	po-lo	(7)	5.5±0.5	750±50	(11)
Madeleine Mine, Gaspe, P.Q.	33.3	17.6	49.5	100.4	33.0	30.4	36.6	EM	po-py	(7)	1.2±0.3	350±50	(13)
Contwoyto L., N.W.T.[5]	33.9	19.0	47.2	100.1	33.2	32.4	34.4	EM	po-lo	(7)		575±25	(14)

Compositions from published d_{131} values were obtained using the equation of Kretschmar & Scott (1976). (EM=electron microprobe, XR=X-ray, WC=wet chemical, ?=possible equilibrium phase). References for Table 1: (1) Present study; (2) Chinn (1969) and present study; (3) Coveney (1972, 1981); (4) Petersen (1983); (5) Brown et al. (1978); (6) Kelly & Turneaure (1970); (7) Kretschmar (1973); (8) Kelly & Rye (1979); (9) Collins (1983); (10) Morimoto & Clark (1961); (11) Phillips & Wall (1981); (12) Kay & Strong (1983); (13) Shelton (1983); (14) Bostock (1968); (15) Walsh et al. (1985); (16) Petersen, pers. comm.

[1]. 0.3 wt.% Co.   [2]. 2.0% Co, 0.3% Ni, 0.1% Sb.   [3]. 0.6% Co, 0.9% Bi, 0.2% Ni.   [4]. Contains Co, Ni, Sb   [5]. 0.1% Co.

composition $FeAs_{1-x}S_{1+x}$, except for one sample where the apparent cation-deficiency is satisfied by cobalt (Fig. 3). No other sample analyzed in this study has appreciable concentrations of elements other than Fe, As or S. Most arsenopyrite grains show small, apparently random, microscopic variations in composition. This same feature has been observed by other investigators (Berglund & Ekström 1980, Lowell & Gasparrini 1982, Kay & Strong 1983, J.K. Bohlke, pers. comm. 1984). No obvious core-to-rim variations were observed in any grains. In addition, no migration or volatilization of elements was detected during microprobe analysis.

Unit-cell data are listed in Table 2 and plotted as composition *versus* volume (Fig. 4) along with the

data of Morimoto & Clark (1961). Our S-rich arsenopyrite data correspond fairly well with those of Morimoto & Clark. For more As-rich compositions, our data indicate a significantly smaller volume (~1%) than the datum of Morimoto & Clark for a synthetic arsenopyrite at 0.564 $X(FeAs_2)$ on the FeS_2–$FeAs_2$ binary join. They noted significant differences in the powder patterns between the synthetic and natural samples and suggested that the synthetic material could probably be indexed using a pseudo-orthorhombic cell (Morimoto & Clark 1961). This higher symmetry is probably due to enhanced disorder and twinning associated wih rapid synthesis and may affect both unit-cell dimensions and d_{131} values. Ignoring this datum, two best-fit curves
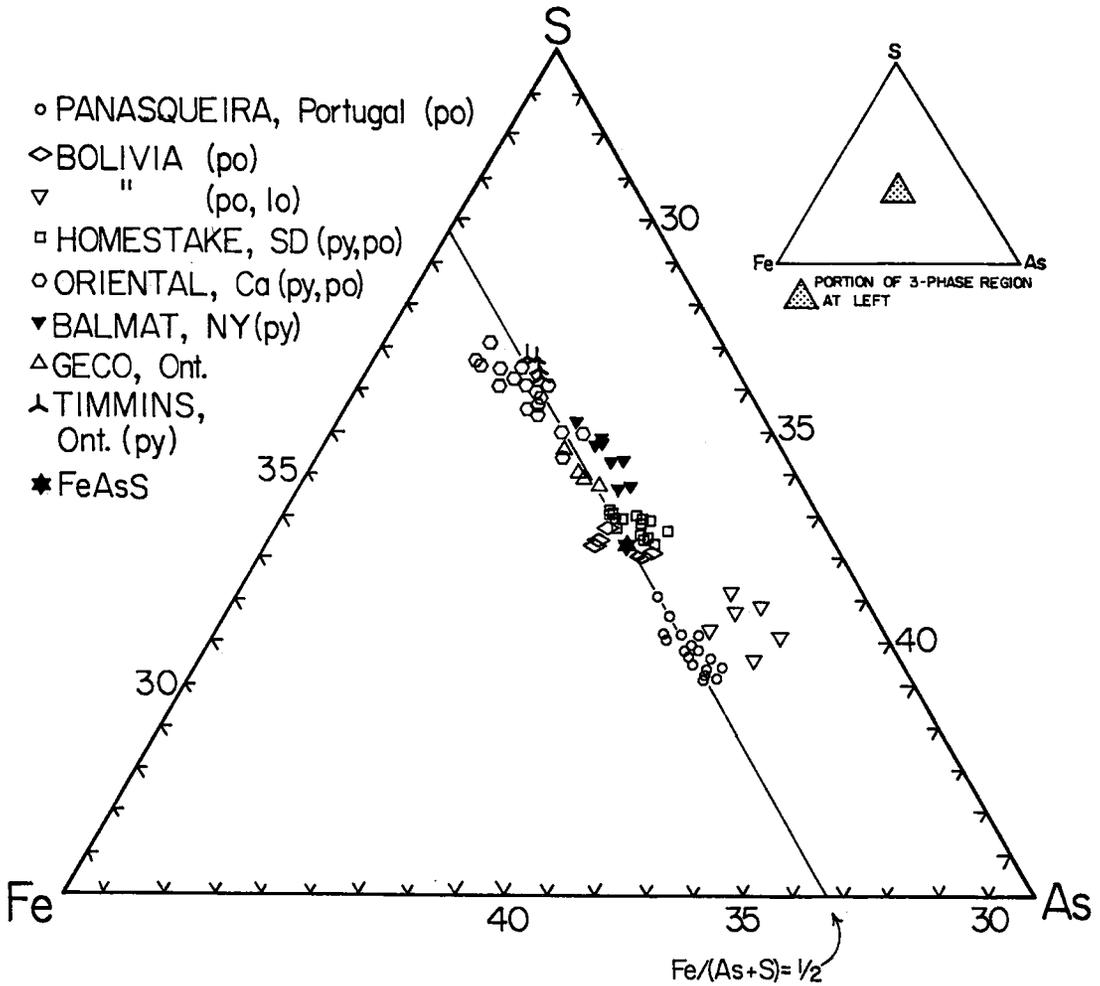
FIG. 3. Arsenopyrite compositions in at.% in the ternary system Fe–As–S. Coexisting phases shown in parentheses.

have been drawn through the remaining data, the first (solid) based only on our new values, and the second (dashed) including the data of Morimoto & Clark (1961) for natural samples.

Comparisons of arsenopyrite compositions determined by electron microprobe and those determined using the d_{131} equation of Kretschmar & Scott (1976) are in excellent agreement (Table 2). For arsenopyrite compositions without appreciable substitution by other elements, the value of d_{131}

appears to be a valid compositional indicator for natural samples.

EXPERIMENTAL AND THERMODYNAMIC CONSIDERATIONS

The stability field of arsenopyrite as a function of $f(S_2)$ and temperature (Fig. 5) (Barton 1969) is bounded by the sulfidation reactions

TABLE 2. CELL PARAMETERS, MOLAR VOLUMES AND CALCULATED d_{131} VALUES FOR ARSENOPYRITE

Sample locality	at.% As in asp (probe)	(X-ray)	a	b	c	β	V^O_{298}	d_{131}
Bolivia (ARA-74)	32.5(3)	32.2	5.748(4)	5.675(2)	5.764(3)	112.04(5)	26.24(3)	1.6308
Bolivia (CHA-23)	33.6(4)	33.5	5.752(3)	5.683(1)	5.779(3)	112.20(3)	26.34(2)	1.6323
Oriental (9-15-112)	29.9(3)	30.9	5.749(3)	5.666(1)	5.757(3)	111.87(3)	26.20(3)	1.6293
Panasqueira (PGL-217)	36.0(5)	35.7	5.767(3)	5.699(1)	5.780(2)	112.46(3)	26.43(3)	1.6348
Panasqueira (PGL-244)	36.5(4)	36.4	5.773(4)	5.702(1)	5.783(3)	112.48(4)	26.48(4)	1.6356

Cell edges and d-values in Angstroms; β in degrees; V in cm³/mole.
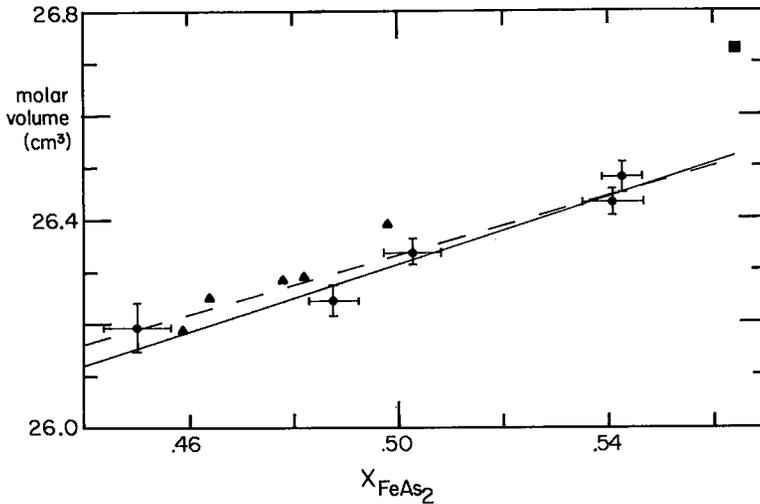
FIG. 4. Volume – composition plot for arsenopyrite. Triangles are from Morimoto
& Clark (1961); circles with error bars are from this study. Errors in the data of
Morimoto & Clark are not shown. Solid best-fit line is for our data exclusively;
dashed line includes data of Morimoto & Clark. The datum for synthetic
arsenopyrite at X FeAs$_2$ = 0.56 (square) is ignored for the fitting of the line.

$$\tfrac{1}{2}S_2 + FeAs_2 + FeS = 2FeAsS \qquad (1)$$

S$_2$ + loellingite + pyrrhotite = arsenopyrite

$$\tfrac{1}{2}S_2 + FeAsS = FeS_2 + As(liq) \qquad (2)$$

S$_2$ + arsenopyrite = pyrite + arsenic liquid

$$\tfrac{1}{2}S_2 + FeAsS = FeS + (As,S)(liq) \qquad (3)$$

S$_2$ + arsenopyrite = pyrrhotite + arsenic–sulfur liquid

$$\tfrac{1}{2}S_2 + FeAsS = FeS_2 + As(s) \qquad (4)$$

S$_2$ + arsenopyrite = pyrite + arsenic metal
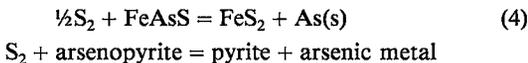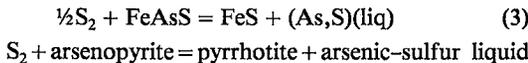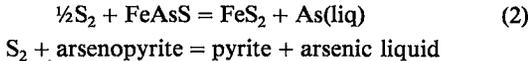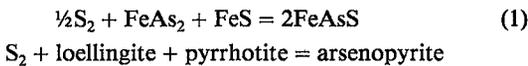
Within the stability field of arsenopyrite, two additional sulfidation reactions

$$\tfrac{1}{2}S_2 + FeS = FeS_2 \qquad (5)$$

S$_2$ + pyrrhotite = pyrite

and

$$\tfrac{1}{2}S_2 + FeAs_2 = FeAsS + As(s) \qquad (6)$$

S$_2$ + loellingite = arsenopyrite + arsenic metal
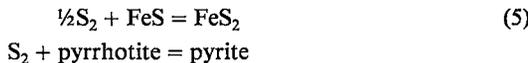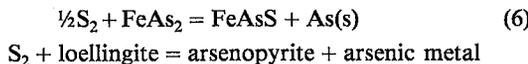
serve to buffer $f(S_2)$ at a given temperature, uniquely defining the composition of a given arsenopyrite in equilibrium with the buffering phases. Whereas other reactions involving As$_2$, H$_2$S, etc., might also be considered, in no way do they invalidate these reactions. We have continued to consider reactions with S$_2$ following Barton (1969, 1970) and Kretschmar & Scott (1976) for direct comparison with their figures. The shift in these

curves with pressure can be estimated using existing thermodynamic data. For the sulfidation curves, the expression

$$\Delta G^P{}_T - \Delta G^\circ{}_T = \int_{1\,bar}^{P} \Delta V_S dP + RT\ln \frac{f(S_2)P}{f(S_2)_{1\ bar}} \qquad (7)$$

can be simplified to

$$\int_{1\,bar}^{P} \Delta V_S dP = RT\ln \frac{f(S_2)_{1\ bar}}{f(S_2)P} \qquad (8)$$

since at equilibrium $\Delta G^P{}_T = 0$ and $f(S_2)_{1\ bar}$ is chosen so that $\Delta G^\circ{}_T = 0$, and the activities of the solid phases are independent of pressure. Unit-cell data for solid solutions of arsenopyrite (Fig. 4) and pyrrhotite (Toulmin & Barton 1964) show a nearly linear dependence of their partial molar volumes with composition, consistent with the assumption of constant activity at all pressures. The ΔV_S for each reaction was calculated at P and T using the computer program EQUILI. Thermodynamic data for all calculations are given in Table 3.

The pressure effect on the melting curves in Figure 5 could not be calculated thermodynamically because of inadequate volume and entropy data for sulfide liquids. A plot of experimentally determined sulfide-melting curves (Fig. 6) shows that the solidus is extended to higher temperatures at higher pressures by an average of $+ 14°C/kbar$. This shift is in excellent agreement with the experimentally determined value of Clark (1960b), but later questioned by Kretschmar & Scott (1976). We have accepted the 14°C/kbar shift in arsenopyrite–pyrite melting curves as a preliminary estimate for the purposes of this
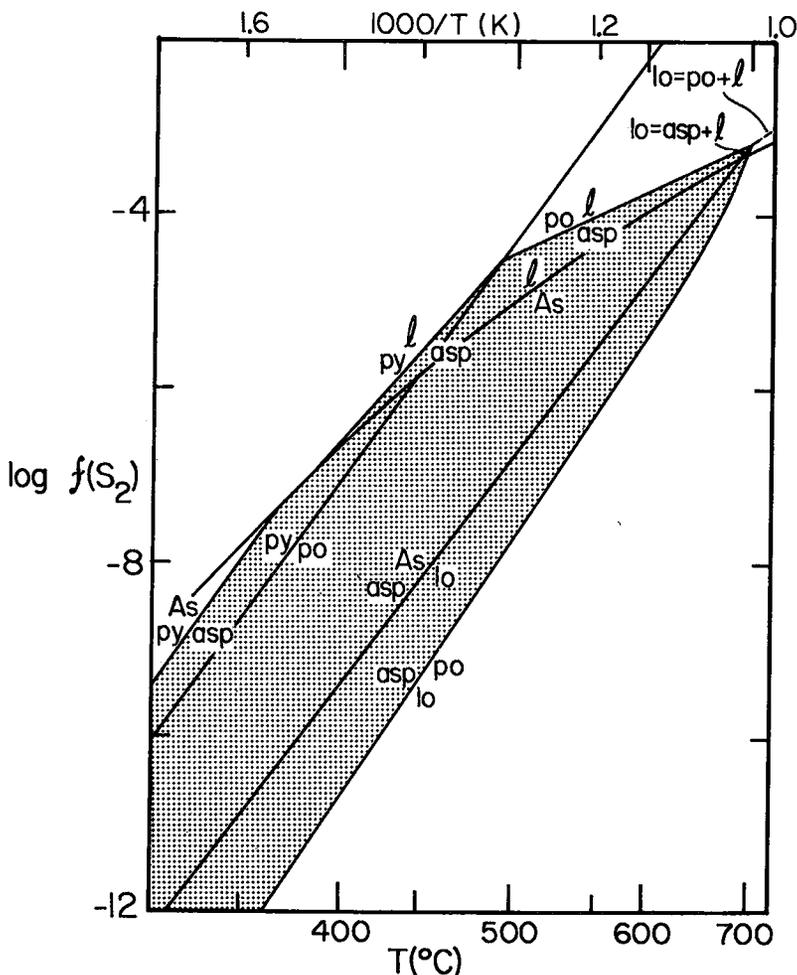
FIG. 5. Sulfidation curves in the system Fe–As–S in the stability range of arsenopyrite (shaded). After Barton (1969).

paper. Using the calculated 5 kbar invariant point for reactions (1) and (6) as a starting point, the stability field of arsenopyrite has been constructed at elevated pressure (Fig. 7). All invariant points are shifted to higher $f(S_2)$ and temperature, although the amount of the shift varies for each reaction. Arsenopyrite may coexist with pyrite up to 550°C at 5 kbar (Fig. 7), significantly higher than the commonly accepted upper limit of 490°C for the stability of arsenopyrite + pyrite at all pressures.

Kretschmar & Scott superimposed their experimentally determined compositional data for arsenopyrite onto Barton's $f(S_2)$–T diagram, connecting equal compositions between buffering curves with straight-line isopleths (Fig. 8). A fixed composition of arsenopyrite in the pyrrhotite field (not buffered by either pyrite or loellingite) defines a univariant curve in $f(S_2)$–T space at constant pressure. Arsenopyrite buffered only by pyrrhotite may lie anywhere along

the isopleth for that specific composition. Arsenopyrite isopleths were extended by Kretschmar & Scott (1976) with a shallow slope into the pyrite and loellingite fields. These fields represent assemblages that include the equilibrium pairs arsenopyrite–pyrite and arsenopyrite–loellingite, respectively. If arsenopyrite lies on the true FeS_2–$FeAs_2$ binary join, its composition will be fixed when buffered by either pyrite or loellingite at constant temperature and pressure. The arsenopyrite compositional isopleths would then have to be vertical in $f(S_2)$–T space in these fields, permitting variations in sulfur fugacity, but not temperature, for a constant composition (Fig. 9). The reaction

$$FeS_2 + \tfrac{1}{2}As_2 = FeAsS + \tfrac{1}{2}S_2 \qquad (9)$$

$$\text{pyrite} + As_2 = \text{arsenopyrite} + S_2$$

illustrates that $\log f(S_2)$ will vary inversely with $\log$

TABLE 3. THERMODYNAMIC DATA USED FOR CALCULATIONS

	V^o_{298}	Source	A	B	C	D	E	Source
Arsenic	12.963	(1)	$1.20X10^{-1}$	$4.97X10^{-3}$	$-2.54X10^{-6}$	$8.42X10^{-9}$	3.16	(5,6)
Arsenopyrite	26.43	(2)	$1.08X10^{-1}$	$4.33X10^{-3}$	$-1.37X10^{-7}$	$9.11X10^{-11}$	0.99	(7,6)
Loellingite	26.67	(3)	$1.10X10^{-1}$	$4.72X10^{-3}$	$2.62X10^{-6}$	$-1.31X10^{-9}$	0.82	(8,9)
Pyrite	23.943	(4)	$6.52X10^{-2}$	$2.54X10^{-3}$	$2.86X10^{-6}$	$-1.82X10^{-9}$	0.69	(4)
Pyrrhotite	18.20	(4)	$4.58X10^{-1}$	$1.89X10^{-2}$	$-2.31X10^{-5}$	$1.39X10^{-8}$	0.12	(4)

V^o_{298} in cm³/mole. For expansivity, $V^o_T = [MV + MV/100(A + BT + CT^2 + DT^3)]$; compressibility
factor $E=1,000(V^o-V) \cdot P^{-1} \cdot V^{-1}$, P in kb. Sources: (1) Robie et al. (1978); (2) Morimoto & Clark
(1961); (3) Ramdohr (1969); (4) Scott (1973); (5) Krishnan et al. (1979) (6) Birch (1966);
(7) Data for CoAs₂. Kjekshus & Rakke (1977), (Isostructural with FeAsS); (8) Kjekshus & Rakke (1977)
(9) Data for mar casite. Birch (1966), (Isostructural with FeAs₂).

$f(As_2)$ in equilibrium with arsenopyrite and pyrite. For a given $a(FeAsS)$ in arsenopyrite, the relationship between sulfur fugacity and arsenic fugacity at constant temperature and pressure is fixed within the stability field of binary arsenopyrite and pyrite. A similar argument applies to binary arsenopyrite and loellingite. The isopleths in the pyrite and loellingite fields in Figure 8 were constructed to fit the experimental results of Kretschmar & Scott (1976) (Fig. 2). The isopleths in the pyrite and loellingite fields would only be vertical if reactions (2), (4) and (5) coincide, and reactions (1) and (6) coincide in Figure 2. If arsenopyrite lies on the pyrite–loellingite binary join, the location of these reactions must coincide. Kretschmar & Scott (1976) attributed the sloping isopleths in the pyrite and loellingite fields to small deviations from the ideal binary join. Slight deviations from the stoichiometric ratio $Fe/(As + S) = \frac{1}{2}$ would place arsenopyrite off the binary join and in the three-phase field Fe–As–S (Fig. 10). Two additional phases would then be required to buffer arsenopyrite, allowing the isopleths in the pyrite and loellingite fields to shift from a vertical slope. However, the very shallowly sloping isopleths in the pyrite- and loellingite-bearing fields (Fig. 8) suggest an even greater dependence on temperature than in the pyrrhotite field. The minor nonstoichiometry observed in arsenopyrite with respect to $Fe/(As + S)$ requires either highly nonideal behavior in arsenopyrite to account for the shallowly sloping isopleths in the pyrite and loellingite fields, or some other explanation. In any case, the assemblage arsenopyrite + pyrrhotite is stable on both sides of reaction (6) in Figure 8. In the absence of loellingite, arsenopyrite isopleths should not change their slope across this boundary. Natural arsenopyrite – loellingite – pyrrhotite assemblages may provide tests of the alternative topologies for arsenopyrite isopleths in the loellingite field, because different temperatures are predicted for this assemblage from each model.

Kretschmar & Scott (1976) determined the location of reaction (6) from their two unreversed experimental data-points at 480° and 550°C (Fig. 2). However, Clark's (1960a) five unreversed arsenopyrite–loellingite–arsenic experiments coincide with
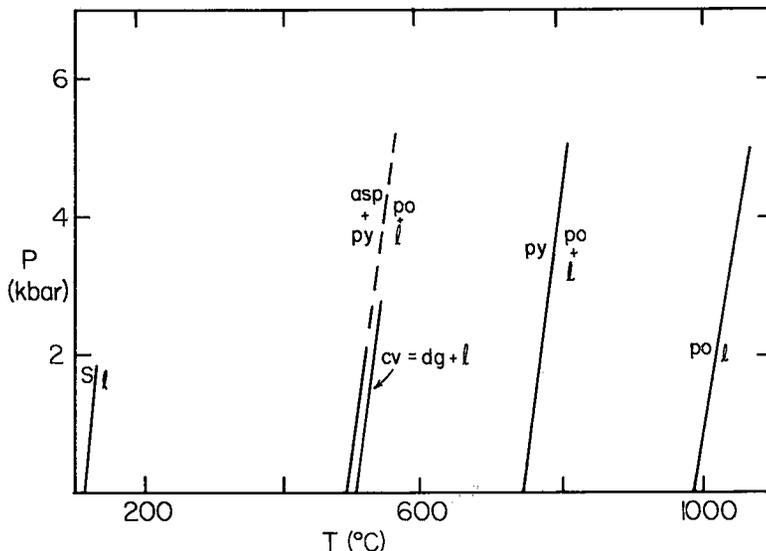
FIG. 6. P–T plot of sulfide melting curves. Data from Clark (1960b), Clark (1966), Kullerud (1964), Ryzhenko & Kennedy (1973). Symbols: cv covellite, dg digenite.
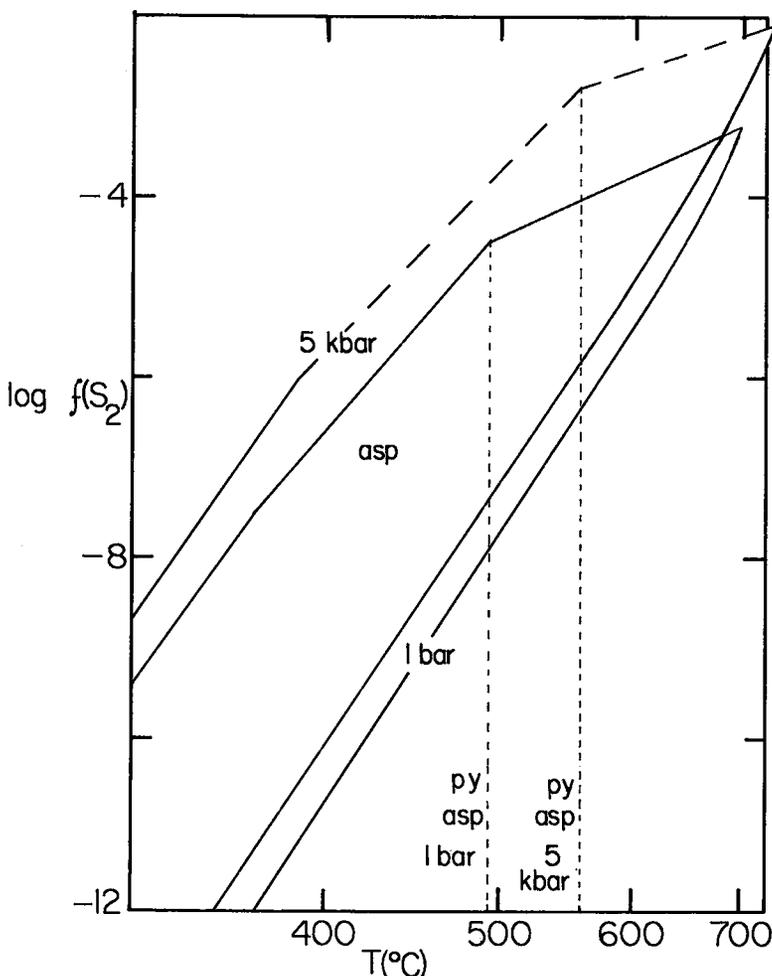
FIG. 7. Stability field of arsenopyrite at 1 bar and at 5 kbar. Also shown is the maximum thermal stability of coexisting pyrite and arsenopyrite at 1 bar and at 5 kbar.

reaction (1) in Figure 2, suggesting that the two curves (1) and (6) may actually coincide. The separation of the two loellingite-bearing curves and the three pyrite-bearing curves (Fig. 2) by Kretschmar & Scott may not be valid, and isopleths may actually be vertical in the pyrite- and loellingite-bearing fields (Fig. 9). Tight compositional reversals are needed to test whether reactions (1) and (6) and reactions (2), (4) and (5) coincide, or whether arsenopyrite shows significant ternary solid-solution, permitting deviation of (1) from (6) and (2) from (5).

If the isopleths in the pyrite and loellingite fields are vertical (Fig. 9), then their positions will be determined by the intersection of the isopleths in the pyrrhotite field with the curves defining the limits of the loellingite and pyrite fields. The shift in the arsenopyrite isopleths in the pyrrhotite field with pressure was calculated from the shift in the reaction

$$FeS + \tfrac{1}{2}S_2 = FeS_2(asp) \qquad (10)$$
$$po + S_2 = FeS_2(asp).$$
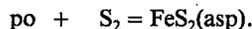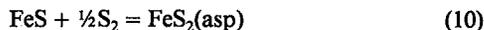
The partial molar volume of FeS_2 in arsenopyrite was determined by extending the unit-cell data in Figure 4 back to end-member FeS_2 (Fig. 11). Whereas the partial molar volume of $FeS_2(asp)$ is still imprecisely known, the available data yield a higher partial molar volume than the molar volume of pyrite. Using 24.85 cm^3/mole for the partial molar volume of FeS_2 in arsenopyrite, the shift of $f(S_2)$ in reaction (10) at 5 kbar and constant temperature was then calculated (Fig. 12). The difference between the $f(S_2)$ shift in reaction (5) and reaction (10) is very small (Fig. 12). The composition of arsenopyrite coexisting with pyrrhotite and pyrite is practically unaffected by pressure, but is shifted by approximately 1 log unit $f(S_2)$ at 5 kbar (Fig. 12). The composition of arsenopyrite coexisting with loel-
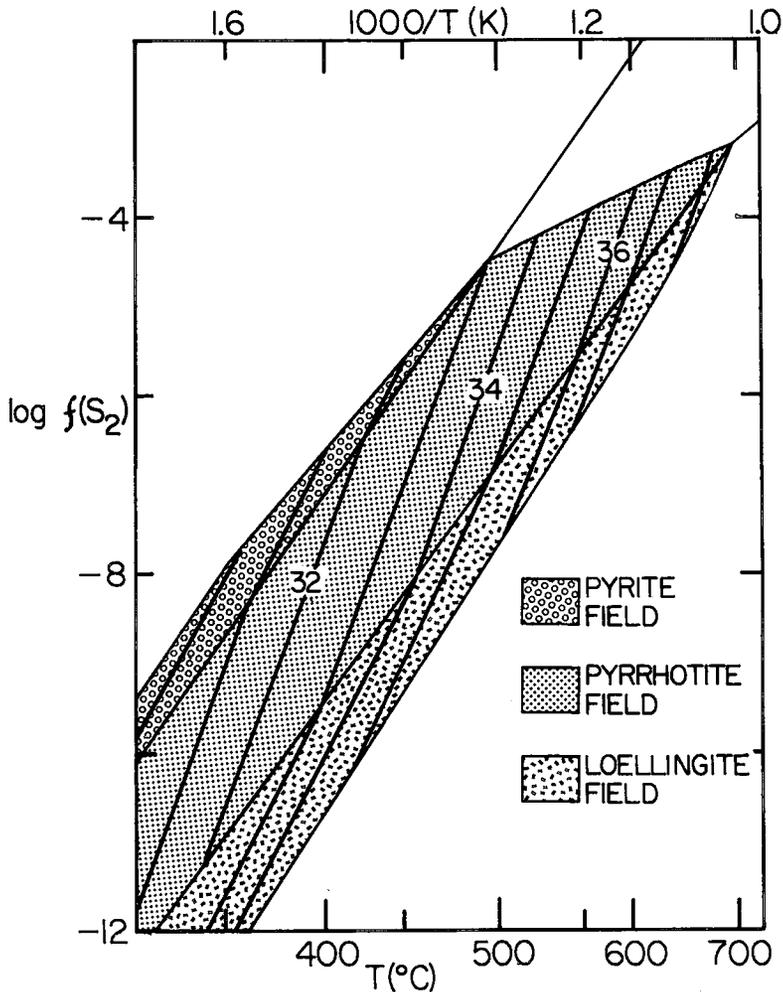
FIG. 8. Isopleths of arsenopyrite composition superimposed on Barton's (1969) $f(S_2)$–T plot (Fig. 5). After Kretschmar & Scott (1976).

lingite is shifted to less As-rich compositions at higher pressures as a result of reaction (6) being shifted more than reaction (5) with increasing pressure (Fig. 12). The shift in the isopleths in Figure 12 is constructed assuming that they retain the same slope at all pressures, but the isopleths could change their slope so as to exactly offset the shift in the arsenopyrite-arsenic–loellingite curve (reaction 6) for all pressures. This cannot be calculated, but there is no reason to expect that the two shifts should exactly coincide. If the change in the slope of the isopleths is minimal, arsenopyrite equilibrated with loellingite at a high pressure will record a low temperature when plotted on the 1 bar isopleth graph of Kretschmar & Scott (Fig. 8). The pressure shift we predict is not very large for any buffered assemblage and should only be considered for high-pressure assemblages. For the assemblage arsenic + arsenopyrite + loellingite

equilibrated at 5 kilobars, the temperature error associated with using the 1 bar calibration of Kretschmar & Scott (1976) will be on the order of 20°C. This small shift is probably less than the precision of the arsenopyrite geothermometer and can be ignored. The shift in sulfur fugacity is not trivial, however, and we suggest that buffered assemblages equilibrated at high pressures have a higher sulfur fugacity ($\sim$0.1 log $f(S_2)$/kbar, *cf.* Fig 12) than predicted by Figure 8.

OBSERVATIONS ON NATURAL ASSEMBLAGES

Arsenopyrite was analyzed from seven localities characterized by varying physicochemical conditions of formation (Table 1). Each locality is described in greater detail below.
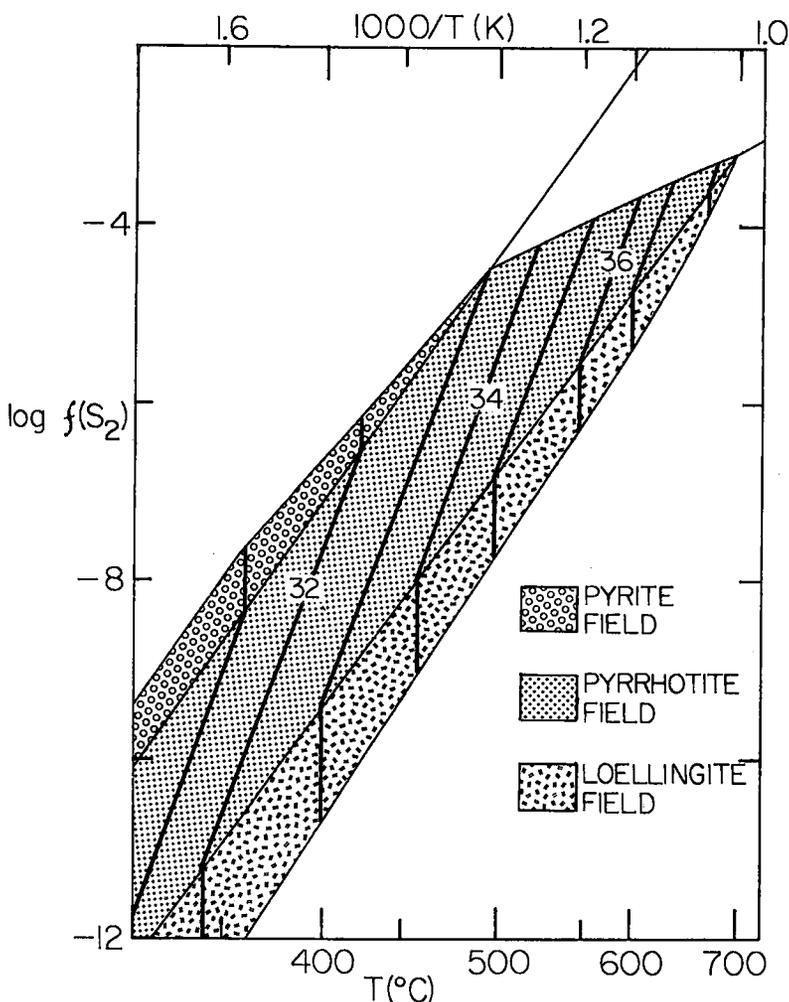
FIG. 9. Isopleths in Figure 8 redrawn vertically in the pyrite and loellingite fields.

Panasqueira, Portugal

The tin–tungsten deposits at Panasqueira are hosted by a sequence of tightly folded pelitic schists (Kelly & Rye 1979). The mineralization occurred in four distinct stages. Arsenopyrite deposition was associated only with the first two stages. In the earliest oxide–silicate stage of mineralization, two events of arsenopyrite deposition are recognized. The main sulfide stage produced arsenopyrite intergrown with pyrrhotite. The third stage of mineralization involved hypogene alteration of pyrrhotite to pyrite and marcasite. The closing stage of mineralization accounts for only very small amounts of sulfide precipitation.

Fluid inclusions from the oxide–silicate stage formed during boiling conditions and need no pressure correction to reconstruct temperatures of for-

mation. Filling temperatures at this stage range from 230° to 360°C, with a cluster of data at 280°C. This corresponds to a pressure of less than 1 kbar (Kelly & Rye 1979). Boiling ceased after the early oxide stage. Filling temperatures do not decrease, however, and Kelly & Rye attributed the lack of boiling in these later inclusions to a reduction of dissolved CO_2 in the fluids rather than to an increase in hydrostatic pressure. Depositional temperatures and pressures are taken as 280 ± 50°C and 1 kbar for the Panasqueira arsenopyrite.

Homestake mine, South Dakota

The Homestake deposit in the Black Hills, South Dakota, consists of intensely deformed Precambrian garnet-biotite schists and retrograde chlorite schists (Slaughter 1968). Compositions of coexisting garnet
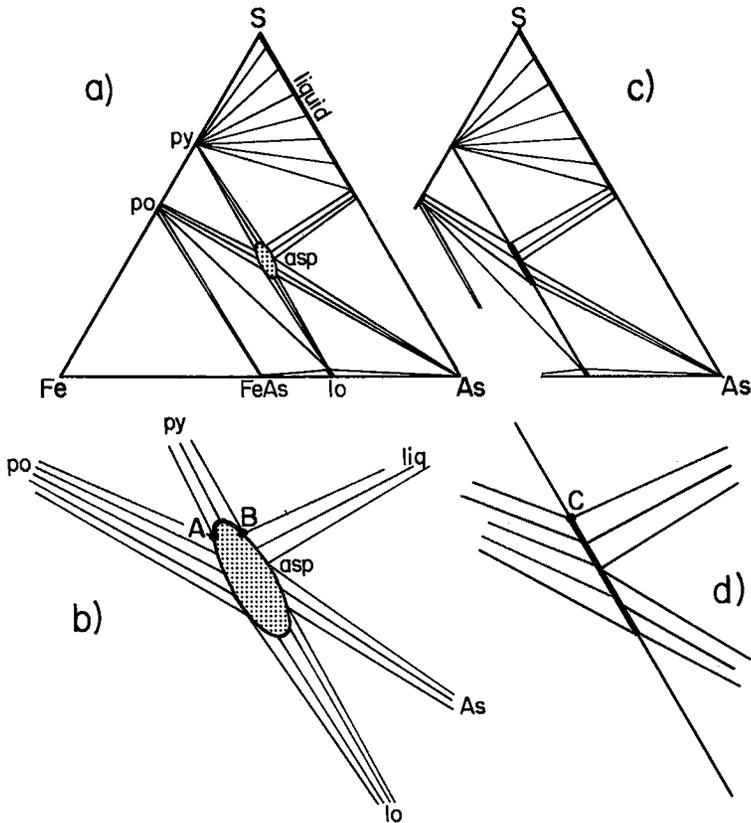
FIG. 10a. Phase relations in the system Fe–As–S between 363 and 491°C (after Kretschmar & Scott 1976). The stability field of arsenopyrite (shaded) is exaggerated to show the effect of slight deviations from the FeS_2–$FeAs_2$ binary join. b. Exploded view of 10a in the region of arsenopyrite. The composition of arsenopyrite in equilibrium with pyrite at a constant pressure and temperature can be anywhere along the bold line between A and B, depending on $f(S_2)$. The composition of arsenopyrite in equilibrium with pyrite and pyrrhotite must lie at A. c,d. Phase relations in the system Fe–As–S for arsenopyrite lying on the binary join FeS_2–$FeAs_2$. In this case, arsenopyrite coexisting with pyrite must lie at point C.

and biotite (Chinn 1969) yield temperatures of 500 ± 50°C using the calibration of Ferry & Spear (1978). Temperatures based on coexisting CO_2- and H_2O-rich fluid inclusions in quartz are 415 ± 15°C, and corresponding pressures are 2.5 ± 0.5 kbar (E. Petersen, pers. comm. 1984). Deposition of arsenopyrite and pyrite occurred at the end of the final event of folding (Noble 1950, Slaughter 1968). Chinn's (1969) textural evidence for equilibrium between garnet, quartz, biotite, cummingtonite and arsenopyrite suggests that temperatures of arsenopyrite formation are close to metamorphic temperatures. Textural evidence suggests the simultaneous crystallization of arsenopyrite, pyrite and pyrrhotite in some samples.

Oriental mine, California

The host rock of the Oriental mine, California,

consists of upper-greenschist-facies metasediments with a few small adjacent granitic intrusive bodies (Coveney 1972, 1981). Arsenopyrite was deposited contemporaneously with pyrite; temperatures of fluid-inclusion homogenization range from 200° to 280°C. Pressure estimates of 0.7 to 2.5 kbar suggest temperatures of formation in excess of 340°, and possibly as high as 500°C (Coveney 1972, 1981). The magnitude of the oxygen-isotope fractionation between mica and quartz is consistent with temperatures of 340 ± 40°C (J.K. Bohlke, pers. comm. 1985).

Bolivia

Mineralization in the tin–tungsten deposits in the Cordillera Real, Bolivia, is associated with a group of small granitic stocks (Kelly & Turneaure 1970). Arsenopyrite formed in the early stages of minerali-

FIG. 11. Extension of unit-cell data on arsenopyrite (Fig. 4) back to end-member FeS_2 and $FeAs_2$; dashed and solid lines have the same slope as in Figure 4. The points labeled py and lo represent the molar volumes of pyrite and loellingite, respectively. Partial molar volume of FeS_2 (asp) used in calculations is the average of the intersections of the dashed and the solid line with the FeS_2 axis.

zation, and is associated with pyrrhotite in all samples and loellingite in sample ARA–107. Fluid-inclusion filling temperatures corrected for pressures of 1.0 kbar correspond to 450–530°C for the early vein-stage event of mineralization (Kelly & Turneaure 1970).

Geco, Ontario

The Geco massive-sulfide deposit, part of the Manitouwadge mining district, northern Ontario, is located in the western Abitibi–Wawa belt and has been studied by Petersen (1983). Petersen's estimates of peak metamorphic conditions are 650 ± 30°C and 6 ± 1 kbar using well-calibrated metamorphic reactions and other geothermometers and geobarometers. These temperatures are slightly higher than the less precise estimates by James *et al.* (1978). The Manitouwadge massive-sulfide deposits were emplaced prior to metamorphism (Friesen *et al.* 1982, Petersen 1983). The single sample of arsenopyrite analyzed consists of four small grains enclosed in an unidentified silver–antimony sulfide.

Timmins, Ontario

The gold deposits near Timmins, Ontario, are hosted in metavolcanic rocks and metagreywackes in the southwestern part of the Abitibi greenstone belt (Smith *et al.* 1984). Mineralization consists of auriferous pyrite disseminated in quartz–carbonate veins, with quartz–pyrite–arsenopyrite deposition occurring in the early stages of vein mineralization (Smith *et al.* 1984). The arsenopyrite–pyrite sample is from the Pamour mine in the eastern part of the Timmins gold region. Temperature and pressure estimates for this deposit are bracketed by the homogenization temperature of the two-phase $(CO_2-CH_4)-H_2O$ fluid inclusions and by the intersection of the (CO_2-CH_4) and $(CO_2-CH_4)-H_2O$ fluid-inclusion isochores (Walsh 1985). These estimates are 320 ± 30°C and 1–1.5 kilobars, broadly consistent with oxygen-isotope temperatures of 400 ± 80°C for the region (Kerrich & Hodder 1982). The arsenopyrite has no detectable minor elements and a low As/(As + S) value, as expected for arsenopyrite equilibrated at a low temperature.

Balmat, New York

Metamorphic temperatures and pressures in the Balmat–Edwards mining district, New York, were determined by Brown *et al.* (1978) using calcite-dolomite thermometry (Goldsmith & Newton 1969) and sphalerite barometry (Scott & Barnes 1971, Scott 1973), and by Bohlen *et al.* (1985) using garnet-rutile–ilmenite–sillimanite–quartz barometry. Their estimates show that the district reached peak temperatures and pressures of 625 ± 25°C and 6.5 ± 0.5 kbar.

FIG. 12. Illustration of the shift in arsenopyrite isopleths at pressure. For simplicity, only the py–po, FeS₂ (asp)–po and lo–asp–As curves are shown (see Fig. 2). The 33% isopleths is shifted to higher $f(S_2)$ when buffered by py–po, and shifted to lower at.%As in asp when buffered by As and lo. Reactions (5) and (10) are shifted by slightly different amounts at 5 kbar, since the partial molar volume of FeS₂ in arsenopyrite is slightly larger than the molar volume of pyrite.

APPLICATION OF THE ARSENOPYRITE
GEOTHERMOMETER TO NATURAL ASSEMBLAGES

Arsenopyrite compositions from this study and others (Morimoto & Clark 1961, Kretschmar 1973, Collins 1983) are plotted on the composition-temperature diagram of Kretschmar & Scott (1976) using temperature estimates from Table 1 (Fig. 13). Uncertainty in the temperature of formation and compositional range of each arsenopyrite sample is illustrated by the size of the sample boxes. Arsenopyrite from all high-grade deposits plots outside the stability field of arsenopyrite. The temperatures predicted by the arsenopyrite compositions in these samples are several hundred degrees *lower* than actual temperatures of formation. These arsenopyrite samples have either reset or are retrograde phases.

Application of the arsenopyrite geothermometer to them is invalid as an indicator of peak metamorphic temperatures. Ore deposits metamorphosed to conditions of the greenschist and lower amphibolite facies plot within the proper compositional fields, but several samples of low-temperature hydrothermal arsenopyrite are unusually As-rich. In particular, arsenopyrite from Panasqueira lies well outside the stability field of arsenopyrite for the temperature of its formation. Applying the phase diagram of Kretschmar & Scott (Fig. 2) to these compositions yields *higher* temperatures than actual temperatures of formation. Kretschmar (1973) reported that arsenopyrite coexisting with pyrite and pyrrhotite from the Madeleine mine contains 36.6 at.% As, contrary to the claim by Kretschmar & Scott (1976) that in all arsenopyrite–pyrite pairs, arsenopyrite
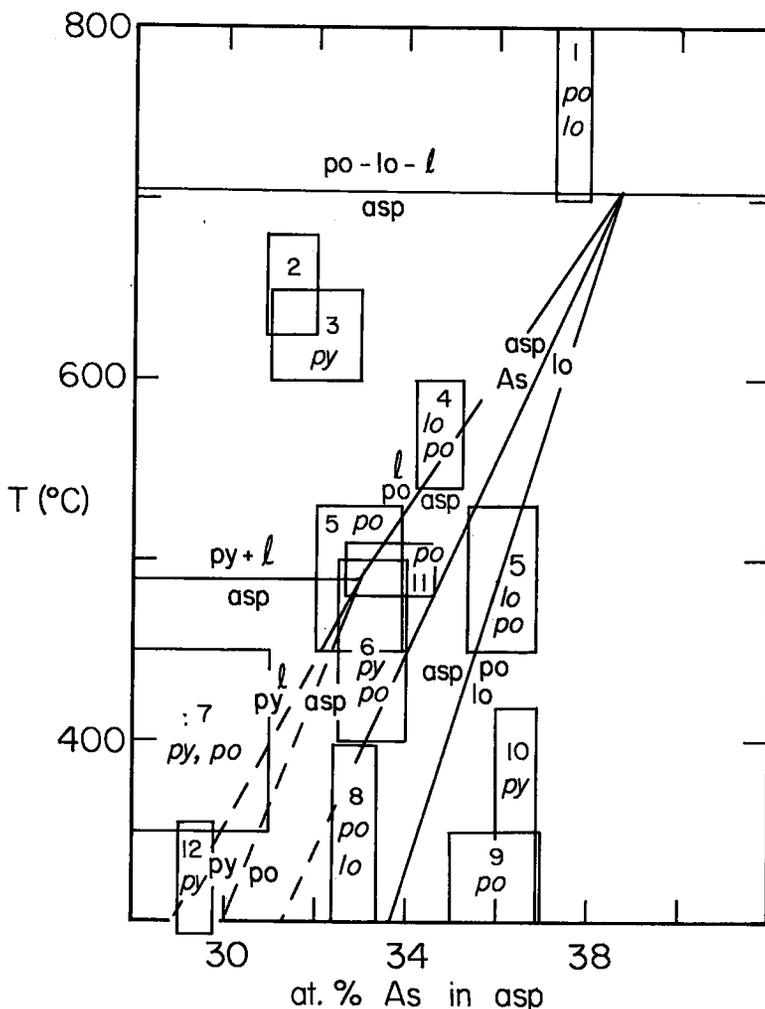
FIG. 13. Assemblage, temperature of formation, and buffering assemblage for various natural samples of arsenopyrite superimposed on Figure 2. 1) Broken Hill, New South Wales, 2) Geco, Ontario, 3) Balmat, New York, 4) Contwoyto Lake, Northwest Territories, 5) Bolivia, 6) Homestake, South Dakota, 7) Oriental, California, 8) Moretons Harbour, Newfoundland, 9) Panasqueira, Portugal, 10) Madeleine, Gaspé, Quebec, 11) Cleveland mine, Tasmania, 12) Timmins, Ontario. The apparently anomalous arsenopyrite compositions from Panasqueira and Madeleine may possibly be explained by change in arsenopyrite isopleths below the hexagonal–monoclinic transition in pyrrhotite (see text).

contains less than 33.3 at.% As. Criteria for equilibrium in hydrothermal deposits are difficult to assess, and apparent equilibrium mineral-assemblages may actually have precipitated metastably under widely fluctuating conditions of supersaturation.

DISCUSSION

The effect of pressure on arsenopyrite composition buffered by two other phases is not large and can be ignored for low-pressure hydrothermal deposits. Pressure will affect the composition of arsenopyrite in metamorphosed deposits, and should not be ignored. The most dramatic effect of pressure is to extend the stability field of coexisting arsenopyrite and pyrite to higher temperatures by approximately 14°C/kbar. The commonly accepted upper limit of 491°C for these two phases is probably incorrect for regional metamorphic assemblages of moderate to high grade.

Arsenopyrite geothermometry has been used for

temperature estimation without additional data from other conventional geothermometers (*e.g.*, Berglund & Ekström 1980, Lowell & Gasparrini 1982, Kay & Strong 1983, Sundblad *et al.* 1984, Kalogeropoulos 1984). Berglund & Ekström (1980) reported on arsenopyrite with $X(As)$ ranging from 31 to 33 mole % coexisting with sphalerite, pyrite and pyrrhotite at five sulfide ore deposits in northern Sweden. Sphalerite barometry (Scott 1983) yields anomalously high pressures (6–8 kbar), and arsenopyrite thermometry give anomalously low temperatures (360–480°C) for rocks associated with middle-amphibolite-facies schists.

Lowell & Gasparrini (1982) applied arsenopyrite geothermometry to samples in equilibrium with pyrite from granite-hosted sulfide veins in southeastern Missouri. The arsenopyrite compositions $X(As)$ cluster at 31.0–32.9 and 32.5–32.9 at.% for two separate veins, corresponding to temperatures of $430 \pm 60°$ and $470 \pm 20°C$, respectively. These estimates are reasonable but have not been checked against other geothermometers.

The compositions of arsenopyrite in hydrothermal veins in the Moretons Harbour Area, Newfoundland (Kay & Strong 1983), are widely scattered [$X(As) = 29$–37 at.%]. Temperature estimates from fluid-inclusion data are $350 \pm 50°C$. The broad range of arsenopyrite compositions is inconsistent with the geothermometer of Kretschmar & Scott since arsenopyrite with $X(As) \geq 34$ at.% is not stable at 350°C.

Sundblad *et al.* (1984) applied arsenopyrite thermometry to several ore deposits in the Swedish Caledonides for samples buffered by pyrite and pyrrhotite. After excluding arsenopyrite with greater than 0.2 wt.% Co, Ni or Sb, they obtained somewhat scattered temperatures of $370 \pm 80°C$ [$X(As)$ 29.5–33.3 at.%] for chlorite-zone deposits and $430 \pm 50°C$ [$X(As)$ 30.8–33.0] for biotite-zone deposits. Whereas these temperatures are in good agreement with thermometers applied to other chlorite- and biotite-zone rocks (*e.g.*, Essene 1982), other well-calibrated thermometers (*e.g.*, calcite-dolomite) should also be applied to these Swedish deposits.

Kalogeropoulos (1984) extrapolated the arseno-pyrite field to 250°C for application of arsenopyrite thermometry to a Pb–Zn massive-sulfide deposit. However, a straight-line extrapolation of the reactions involving arsenopyrite and pyrite in Figure 2 is not valid (Kretschmar & Scott 1976). Arsenopyrite compositional data suggesting low temperatures of formation are inconclusive without independent thermometric evidence. Sphalerite isopleths change radically below the hexagonal–monoclinic transition in pyrrhotite (Scott & Kissin 1973). The pyrrhotite transition may cause the arsenopyrite reaction-curves (Fig. 2) to shift to more As-rich compositions at low

temperatures, thereby fitting the arsenopyrite data from the anomalous hydrothermal deposits (Fig. 13).

Arsenopyrite geothermometry appears to be valid for ore deposits metamorphosed at low or intermediate grades, but the accuracy is less than desirable. The range of compositions analyzed within a single sample may be too broad to reasonably constrain temperatures of formation. The compositions reported by Kay & Strong (1983) for arsenopyrite from Moretons Harbour, Newfoundland range from 29 to 36 at.% As, spanning the entire known compositional range of arsenopyrite. Arsenopyrite apparently buffered by pyrite and pyrrhotite at the Homestake mine ranges from 32.5 to 34.0 at.% As, equivalent to a temperature range of 465° to 535°C. The composition of arsenopyrite coexisting with pyrite and pyrrhotite from the Oriental mine, California, only limits temperatures to less than 400°C. The arsenopyrite + pyrrhotite + loellingite assemblage from Bolivia limits temperatures to between 490° and 610°C. Coexisting arsenopyrite and pyrrhotite restrict temperature to a lesser degree. The composition of arsenopyrite from Bolivia buffered by pyrrhotite constrains temperatures to less than 525°C. The coexistence of arsenopyrite from Panasqueira with pyrrhotite indicates temperatures between 410° and 635°C, whereas actual temperatures of formation as assessed by fluid-inclusion data are less than 350°C. The arsenopyrite + pyrite assemblage from Timmins limits temperature to less than 330°C.

Application of the arsenopyrite geothermometer to samples formed under conditions other than greenschist and amphibolite facies is not recommended. Arsenopyrite from high-grade metamorphic rocks appears to have reset, and arsenopyrite from hydrothermal deposits may not have attained equilibrium. Wide compositional ranges of arsenopyrite have been interpreted as effects of temperature variation or fluctuation in sulfur fugacity within the hydrothermal system (Lowell & Gasparrini 1982, Kalogeropoulos 1984). Berglund & Ekström (1980) proposed that local $f(S_2)$ variations exist in medium-grade metamorphic rocks, based on varying compositions of arsenopyrite on a fine scale. We suggest that the arsenopyrite geothermometer be used with discretion, preferably in conjunction with other, better-calibrated thermometers (*e.g.*, Essene 1982) Tightly reversed experiments are still needed before the arsenopyrite geothermometer can be regarded as fully quantified. Unfortunately, there are few calibrated geothermometers other than the arsenopyrite geothermometer that can be applied to massive-sulfide deposits. An understanding of the low-temperature behavior of arsenopyrite and the effect of minor-element substitution would be valuable. These topics, combined with new high-pressure experiments involving compositional reversals,

should be the focus of further investigations in the system Fe–As–S.

REFERENCES

BARTON, P.B., JR. (1969): Thermochemical study of the system Fe–As–S. *Geochim. Cosmochim. Acta* 33, 841-857.

———— (1970): Sulfide petrology. *Mineral Soc. Amer. Spec. Pap.* 3, 187-198.

BERGLUND, S. & EKSTRÖM, T.K. (1980): Arsenopyrite and sphalerite as T–P indicators in sulfide ores from northern Sweden. *Mineral. Deposita* 15, 175-187.

BIRCH, F. (1966): Compressibility; elastic constants. *In* Handbook of Physical Constants (S.P. Clark Jr., ed.). *Geol. Soc. Amer. Mem.* 97, 97-173.

BOHLEN, S.R., VALLEY, J.W. & ESSENE, E.J. (1985): Metamorphism in the Adirondacks. I. Pressure and temperature. *J. Petrology* 26, (in press).

BOSTOCK, H.S. (1968): Gold – arsenopyrite – loellingite – pyrrhotite deposits in amphibolite, Itchen Lake – Contwoyto Lake area, District of Mackenzie. *Geol. Surv. Can. Pap.* 68-1B, 72-76.

BROWN, P.E., ESSENE, E.J. & KELLY, W.C. (1978): Sphalerite geobarometry in the Balmat–Edwards district, New York. *Amer. Mineral.* 63, 250-257.

BURNHAM, C.W. (1961): Lattice constant refinement. *Carnegie Inst. Wash. Year Book* 61, 132-135.

CHINN, W. (1969): *Structural and Mineralogical Studies at the Homestake Mine, Lead, South Dakota.* Ph.D. dissertation, Univ. California, Berkeley, California.

CLARK, L.A. (1960a): The Fe–As–S system: phase relations and applications. *Econ. Geol.* 55, 1345-1381, 1631-1652.

———— (1960b): The Fe–As–S system. Variations of arsenopyrite compositions as a function of T and P. *Carnegie Inst. Wash. Year Book* 59, 127-130.

CLARK, S.P., JR. (1966): High-pressure phase equilibria. *In* Handbook of Physical Constants (S.P. Clark Jr., ed.). *Geol. Soc. Amer. Mem.* 97, 345-370.

COLLINS, P.L.F. (1983): *Geology and Mineralisation at the Cleveland Mine, Western Tasmania.* Ph.D. dissertation, Univ. Tasmania, Hobart, Australia.

COVENEY, R.M. (1972): *Gold Mineralization at the Oriental Mine, Alleghany, California.* Ph.D. dissertation, Univ. Michigan, Ann Arbor, Mich.

———— (1981): Gold quartz veins and auriferous granite at the Oriental mine, Alleghany District, California. *Econ. Geol.* 76, 2176-2199.

ESSENE, E.J. (1982): Geologic thermometry and barometry. *In* Characterization of Metamorphism Through Mineral Equilibria (J.M. Ferry, ed.). *Mineral. Soc. Amer., Rev. Mineral.* 10, 153-206.

FERRY, J.M. & SPEAR, F.S. (1978): Experimental calibration of the partitioning of Fe and Mg between biotite and garnet. *Contr. Mineral. Petrology* 66, 113-117.

FRIESEN, R.G., PIERCE, G.A. & WEEKS, R.M. (1982): Geology of the Geco base metal deposit. *In* Precambrian Sulphide Deposits (R.W. Hutchinson, C.D. Spence & J.M. Franklin, eds.). *Geol. Assoc. Can. Spec. Pap.* 25, 343-363.

GOLDSMITH, J.R. & NEWTON, R.C. (1969): P–T–X relations in the system $CaCO_3$–$MgCO_3$ at high temperatures and pressures. *Amer. J. Sci.* 267-A, 160-190.

JAMES, R.S., GRIEVE, R.A.F. & PAUK, L. (1978): The petrology of cordierite–anthophyllite gneisses and associated mafic and pelitic gneisses at Manitouwadge, Ontario. *Amer. J. Sci.* 278, 41-63.

KALOGEROPOULOS, S.I. (1984): Composition of arsenopyrite from the Olympias Pb–Zn massive sulfide deposit, Chalkidiki Peninsula, N. Greece. *Neues Jahrb. Mineral. Monatsh.*, 296-300.

KAY, A. & STRONG, D.F. (1983): Geologic and fluid controls on As–Sb–Au mineralization in the Moretons Harbour area, Newfoundland. *Econ. Geol.* 78, 1590-1604.

KELLY, W.C. & RYE, R.O. (1979): Geologic, fluid inclusion, and stable isotope studies of the tin-tungsten deposits of Panasqueira, Portugal. *Econ. Geol.* 74, 1721-1822.

———— & TURNEAURE, F.S. (1970): Mineralogy, paragenesis and geothermometry of the tin and tungsten

deposits of the eastern Andes, Bolivia. *Econ. Geol.* **65**, 609-680.

KERRICH, R. & HODDER, R.W. (1982): Archean lode gold and base metal deposits; chemical evidence for metal separation into independent hydrothermal systems. *Can. Inst. Mining Metall. Spec. Vol.* **24**, 144-160.

KJEKSHUS, A. & RAKKE, T. (1977): High temperature studies of marcasite and arsenopyrite type compounds. *Acta Chem. Scand.* **A 31**, 517-529.

KLEMM, D.D. (1965): Synthesen und Analysen in den Dreiecksdiagrammen FeAsS–CoAsS–NiAsS und FeS$_2$–CoS$_2$–NiS$_2$. *Neues Jahrb. Mineral. Abh.* **103**, 205-255.

KRETSCHMAR, U. (1973): *Phase Relations Involving Arsenopyrite in the System Fe–As–S and Their Application*. Ph.D. thesis, Univ. Toronto, Toronto, Ont.

_____ & SCOTT, S.D. (1976): Phase relations involving arsenopyrite in the system Fe–As–S and their application. *Can. Mineral.* **14**, 364-386.

KRISHNAN, R.S., SRINIVASAN, R. & DEVANARAYANAN, S. (1979): *Thermal Expansion of Crystals*. Pergamon Press, London.

KULLERUD, G. (1964): Review and evaluation of recent research on geologically significant sulfide-type systems. *Fortschr. Mineral.* **41**, 221-270.

LOWELL, G.R. & GASPARRINI, C. (1982): Composition of arsenopyrite from topaz greisen veins in southeastern Missouri. *Mineral. Deposita* **17**, 229-238.

MORIMOTO, N. & CLARK, L.A. (1961): Arsenopyrite crystal-chemical relations. *Amer. Mineral.* **46**, 1448-1469.

NOBLE, J.A. (1950): Ore mineralization in the Homestake gold mine, Lead, South Dakota. *Geol. Soc. Amer. Bull.* **61**, 221-252.

PETERSEN, E.U. (1983): *Metamorphism and Geochemistry of the Geco Massive Sulfide Deposit and its Enclosing Wall-rocks*. Ph.D. thesis, Univ. Michigan, Ann Arbor, Mich.

PHILLIPS, G.N. & WALL, V.J. (1981): Evaluation of prograde regional metamorphic conditions: their implications for the heat source and water activity during metamorphism in the Willyama Complex, Broken Hill, Australia. *Bull. Minéral.* **104**, 801-810.

RAMDOHR, P. (1969): *The Ore Minerals and their Intergrowths*. Pergamon Press, London.

RYZHENKO, B. & KENNEDY, G.C. (1973): The effect of pressure on the eutectic in the system Fe–FeS. *Amer. J. Sci.* **273**, 803-810.

ROBIE, R.A., HEMINGWAY, B.S. & FISHER, J.R. (1978): Thermodynamic properties of minerals and related substances at 298.15 K and 1 bar (10^5 Pascals) pressure and at higher temperatures. *U.S. Geol. Surv. Bull.* **1452** (revised edition).

SCOTT, S.D. (1973): Experimental calibration of the sphalerite geobarometer. *Econ. Geol.* **68**, 466-474.

_____ (1974): Experimental methods in sulfide synthesis. *In* Sulfide Mineralogy (P.H. Ribbe, ed.). *Mineral. Soc. Amer., Rev. Mineral.* **1**, S1-38.

_____ (1976): Application of the sphalerite geobarometer to regionally metamorphosed terrains. *Amer. Mineral.* **61**, 661-670.

_____ (1983): Chemical behaviour of sphalerite and arsenopyrite in hydrothermal and metamorphic environments. *Mineral. Mag.* **47**, 427-435.

_____ & BARNES, H.L. (1971): Sphalerite geothermometry and geobarometry. *Econ. Geol.* **66**, 653-669.

_____ & KISSIN, S.A. (1973): Sphalerite composition in the Zn–Fe–S system below 300°C. *Econ. Geol.* **68**, 475-479.

SHELTON, K.L. (1983): Composition and origin of ore-forming fluids in a carbonate-hosted porphyry copper and skarn deposit: a fluid inclusion and stable isotope study of Mines Gaspé, Québec. *Econ. Geol.* **78**, 387-421.

SLAUGHTER, A.L. (1968): The Homestake mine. *In* Ore Deposits of the United States (J.D. Ridge, ed.). *Amer. Inst. Mining Metall. Petroleum Engin.*, 1436-1459.

SMITH, T.J., CLOKE, P.L. & KESLER, S.E. (1984): Geochemistry of fluid inclusions from the McIntyre–Hollinger gold deposit, Timmins, Ontario, Canada. *Econ. Geol.* **79**, 1265-1285.

SUNDBLAD, K., ZACHRISSON, E., SMEDS, S.-A., BERGLUND, S. & ALINDER, C. (1984): Sphalerite geobarometry and arsenopyrite geothermometry applied to metamorphosed sulfide ores in the Swedish Caledonides. *Econ. Geol.* **79**, 1660-1668.

TOULMIN, P., III & BARTON, P.B., JR. (1964): A thermodynamic study of pyrite and pyrrhotite. *Geochim. Cosmochim. Acta* **28**, 641-671.

WALSH, J.F. (1985): *Physical and Chemical Controls on Gold Mineralization at the Pamour #1 Mine, Timmins, Ontario, Canada*. M.S. thesis, Univ. Michigan, Ann Arbor, Mich.